

Photoelectric response of a gold electrode modified with self-assembled monolayers of pyrrolidinofullerenes

Sheng Zhang,^a Dong Dong,^b Liangbing Gan,^{*a} Zhongfan Liu^b and Chunhui Huang^a

^a State Key Lab of Rare Earth Materials Chemistry and Applications, Peking University, Beijing 100871, China

^b Center for Nanoscale Science & Technology, Department of Chemistry, Peking University, Beijing 100871, China. E-mail: gan@chem.pku.edu.cn; Fax: + 86-10-62751708; Tel: + 86-10-62757957

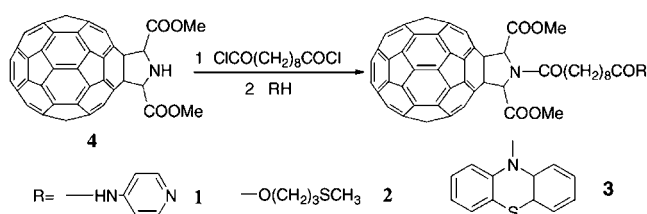
Received (in Montpellier, France) 4th September 2000, Accepted 22nd January 2001

First published as an Advance Article on the web 19th March 2001

Three new fullerene derivatives **1**, **2** and **3** have been synthesized, which can form stable self-assembled monolayers (SAMs) on a gold surface. These SAMs were characterized by contact angle measurements and scanning tunneling microscopy. The photoelectric conversion properties of the SAMs have also been investigated. Photocurrent action spectra show that the excited fullerene derivatives **1**, **2** and **3** act as photoactive species in the photoinduced electron transfer process. Factors such as intensity of irradiation and bias voltage have been studied. The quantum yields of the SAMs range from 2.9 to 14.9% under the most favorable conditions.

Due to their unique electronic, spectroscopic and structural properties, fullerenes have been widely studied since their discovery in 1985.¹ Fullerenes are strong electron acceptors and electron transfer from various electron donors to photoexcited C₆₀ has been reported.^{2,3} Photoelectroactive fullerene derivatives, such as porphyrin–fullerene⁴ and ruthenium complex–fullerene dyads,⁵ exhibit ultrafast intramolecular electron transport. The C₆₀ moiety has been found to act as an effective electron acceptor in C₆₀ ferrocene-based dyads.⁶

Thin films of fullerenes have been prepared using a number of strategies including gas-phase deposition,⁷ Langmuir–Blodgett⁸ and self-assembly⁹ techniques. Self-assembled monolayers, mainly obtained from thiol derivatives on Au surfaces, are useful for constructing highly ordered, two- and three-dimensional structures on substrates.¹⁰ Dominguez and Echegoyen have reported that bipyridine and pyridyl compounds adsorb strongly on Au surfaces in much the same way as thiols do.¹¹ Several groups have already reported the preparation, electrochemistry and surface properties of C₆₀ SAMs. We have reported the photoelectric conversion properties of fullerene derivatives by using Langmuir–Blodgett (LB) technology.^{12–14} However, studies on the photoelectric conversion properties of C₆₀ SAMs are still rare.¹⁵ To the best of our knowledge, there have been no reports on the photoelectrochemical properties of SAMs formed by nitrogens of pyridyl compounds adsorbed on a Au surface. Here we report the photoelectrochemical behavior of SAMs of compounds **1–3** shown in Scheme 1.



Scheme 1

Experimental

Spectroscopic, photoelectrochemical and electrochemical measurements

The elemental analyses were carried out with a Carlo Erba 1106 elemental analyser. The NMR spectra were recorded on a Bruker ARX 400 spectrometer. The absorption spectra were measured with a Shimadzu UV-3100 spectrophotometer. Cyclic voltammetry was measured using the same conditions as we reported previously.¹⁶ The photoelectrochemical studies were performed by using a model 600 voltammetry analyzer (CH Instruments, USA) and a 500 W xenon lamp (USHIO Electric, Japan). An IRA-25S filter was always used to avoid thermal effects throughout all experiments. A three-electrode cell having a flat window for illumination of the working electrode was used. The counter electrode was a Pt wire and the reference was a saturated calomel electrode (SCE). KCl solution (0.1 M) containing the electron donor (H₂Q) was used as the electrolyte solution.

Materials

Hydroquinone (H₂Q) was AR grade and used without further purification. Phenothiazine, 3-(methylthio)-1-propanol, 4-aminopyridine and sebacoyl chloride were purchased from ACROS Chemical Co. Pyridine was AR grade. Toluene was purified by refluxing with Na. Chloroform was purified by distillation over P₂O₅. Deionized water, purified by passing through an Easy Pure RF Compact Ultrapure Water System (Barnstead Co., USA), was used throughout all experiments. Fullerene derivative **4** was prepared by irradiation of glycine methyl ester or iminodiacetic methyl ester with C₆₀, as we reported previously.¹⁷

Synthesis of compounds **1**, **2** and **3**

Syntheses of compounds **1**, **2** and **3** were carried out as shown in Scheme 1. The following describes the synthesis of compound **3** as an example.

Preparation of 3. Sebacoyl chloride (300 mg, 1.26 mmol) was added at room temperature to a stirred solution of **4** (85 mg, 0.10 mmol) and pyridine (2 ml) in freshly distilled dry toluene (100 ml), which was under nitrogen and protected from light with an aluminum foil. After the mixture was stirred for 24 h, phenothiazine (530 mg, 2.66 mmol) was added at room temperature to the reaction mixture and stirred for another 8 h. The red-brown solution was evaporated. The residue was extracted with toluene and chromatographed on silica gel. Toluene first eluted a small portion of unreacted **4**. The product band was washed out with chloroform. The solvent was evaporated and the residue was washed with methanol and petroleum ether and then dried under vacuum to give **3** as a brown powder (92% yield). ^1H NMR (200 MHz, CDCl_3): δ 1.30–1.70 (m, 10H), 1.70–2.00 (m, 2H), 2.46 (t, 2H, $J = 7.2$), 2.79 (t, 2H, $J = 7.2$ Hz), 3.93 (s, 6H), 6.57 (s, 2H), 7.20–7.58 (m, 8H). ^{13}C NMR (100 MHz, CDCl_3): δ 172.44, 172.17, 168.96, 153.51, 150.16, 147.45, 146.36, 146.32, 146.09, 146.05, 145.71, 145.58, 145.50, 145.47, 145.45, 145.32, 145.26, 144.41, 144.37, 144.23, 143.15, 143.08, 142.69, 142.61, 142.24, 142.06, 142.02, 141.79 (br), 141.76, 140.16, 139.58, 138.82, 137.38, 134.07, 133.23, 128.89, 127.96, 127.29, 126.93, 126.74, 71.14, 70.15, 52.94, 34.31, 34.19, 29.25, 29.20, 29.16, 29.00, 25.27, 24.98. MALDI-TOF (m/z): 1283 (6, $\text{M}^+ + \text{K}$), 1267 (84, $\text{M}^+ + \text{Na}$), 880 (8), 820 (21), 720 (100%, C_{60}^+). UV-Vis: λ 256, 314, 431 nm. Anal. calc. for $\text{C}_{88}\text{H}_{32}\text{O}_6\text{N}_2\text{S}$: C 84.88; H 2.59; N 2.25; found: C 84.53; H 2.67; N 1.93%.

Preparation of 1. **1** was prepared as for **3**, yield 52%. ^1H NMR (200 MHz, CDCl_3): δ 1.30–1.80 (m, 10H), 1.80–2.00 (m, 2H), 2.50 (t, 2H, $J = 7.2$), 2.83 (t, 2H, $J = 7.2$ Hz), 3.94 (s, 6H), 6.57 (s, 2H), 7.60–7.80 (m, 2H), 8.35–8.42 (s, 2H), 8.45 (s, 1H). ^{13}C NMR (100 MHz, CDCl_3): δ 172.68, 172.45, 169.03, 153.51, 150.34, 150.06, 147.57, 146.48, 146.42, 146.22, 146.17, 145.73, 145.69, 145.63, 145.56, 145.54, 145.42, 145.37, 144.50, 144.45, 144.26, 143.26, 143.19, 142.81, 142.75, 142.31, 142.13, 142.06, 141.89, 141.84 (br), 140.27, 139.69, 137.41, 134.10, 113.63, 70.35, 53.02, 37.69, 34.37, 29.08, 29.04, 28.98, 25.20, 24.92. MALDI-TOF (m/z): 1162 (51, $\text{M}^+ + \text{Na}$), 1140 (61, $\text{M}^+ + 1$), 720 (100%, C_{60}^+). UV-Vis: λ 257, 313, 431 nm. Anal. calc. for $\text{C}_{81}\text{H}_{29}\text{O}_6\text{N}_3 \cdot 0.5\text{CHCl}_3 \cdot \text{H}_2\text{O}$: C 80.98; H 2.54; N 3.48; found: C 80.54; H 2.63; N 3.42%.

Preparation of 2. **2** was prepared as for **3**, yield 87%. ^1H NMR (200 MHz, CDCl_3): δ 1.30–1.74 (m, 10H), 1.80–2.05 (m, 4H), 2.11 (s, 3H), 2.31 (t, 2H, $J = 7.2$), 2.50–2.66 (m, 2H), 2.82 (t, 2H, $J = 7.2$), 3.94 (s, 6H), 4.17 (t, 2H, $J = 6.6$ Hz), 6.54 (s, 2H). ^{13}C NMR (100 MHz, CDCl_3): δ 173.71, 172.42, 168.99, 153.53, 150.17, 147.49, 146.40, 146.39, 146.14, 146.09, 145.73, 145.63, 145.54, 145.51, 145.48, 145.36, 145.30, 144.45, 144.41, 144.27, 143.19, 143.12, 142.73, 142.66, 142.27, 142.09, 142.05, 141.83 (br), 141.79, 140.19, 139.62, 137.40, 134.11, 71.20, 70.15, 62.81, 52.98, 34.35, 30.61, 29.32, 29.24, 29.16, 29.03, 28.21, 24.99, 24.94, 15.52. MALDI-TOF (m/z): 1190 (38, $\text{M}^+ + \text{K}$), 1174 (20, $\text{M}^+ + \text{Na}$), 720 (100%, C_{60}^+). UV-Vis: λ 256, 313, 431 nm. Anal. calc. for $\text{C}_{80}\text{H}_{33}\text{O}_7\text{NS}$: C 83.39; H 2.89; N 1.22; found: C 83.00; H 2.72; N 1.15%.

Preparation of SAMs

Gold substrates were prepared by sputter-coating glass plates, which were pretreated by soaking at 95 °C for 20 min in “piranha” solution (7 : 3 H_2SO_4 – H_2O_2), with a 10 nm Ti adhesion layer and 200 nm Au layer. **Caution!** “Piranha” solution should be handled carefully because of its violent reactivity with organic materials. The gold-coated plates were cut into slides (1.5 × 2.4 cm). After being soaked at 95 °C for 5 min in “piranha” solution, the gold slides were washed with deionized water and absolute ethanol and then dried under a flow of nitrogen. The clean gold slides were immediately immersed

in solutions (0.1 mM) of compounds **1**, **2** or **3** in CHCl_3 . All adsorptions were allowed to equilibrate for a period of 2 days. The resulting SAMs were exhaustively rinsed with chloroform and ethanol, and dried under a flow of nitrogen before characterization.

Characterization of SAMs

Scanning tunneling microscopy (STM) measurements were carried out under ambient conditions with a Nanoscope III_A (Digital Instruments, Santa Barbara, CA). Scanners E and A were used for scanning on scales from 1 μm to 20 nm in the constant current mode. Mechanically cut Pt/Ir (80 : 20) tips were used. Atomically flat Au(111) was obtained by using the flame melting method.

Contact angles were measured using a Rudolf Research Auto El III ellipsometer equipped with a He-Ne laser operating at a wavelength of 632.8 nm. The data were collected and averaged over three separate slides. The contact angles of H_2O on SAMs derived from compounds **1**, **2** and **3** were 73, 72 and 70°, respectively, and that of bare gold was 50°.

In principle, the fullerene derivatives can be reduced stepwise with up to six electrons. The CV spectrum of the SAM of compound **2** gave only the first reduction and oxidation peaks. Further reduction signals were not recognizable. From these data, an approximate surface coverage Γ 1.2×10^{-10} mol cm^{-2} (137 \AA^2 molecule $^{-1}$) can be derived. The CV spectra of the SAMs of compounds **1** and **3** gave broad humps at the expected first reduction and oxidation potentials. It was not possible to obtain accurate surface coverage values from these spectra.

Procedure for the estimation of absorbance of the SAMs

Due to their low absorbances the absorption spectra of the SAMs of compounds **1**, **2** and **3** could not be obtained accurately in the reflection mode. Instead, the following procedure was applied to estimate the absorbances of these SAMs.

The UV-Vis spectrum of a chloroform solution of the compound with known concentration (of the order of 10^{-5} M) is measured. The absorbance (A_1) of the solution at a given wavenumber can thus be obtained. The number of molecules (M_1) responsible for the UV-Vis spectrum is then calculated by using the concentration and the specific volume measured in the spectrometer. This specific volume is the light path area (the window) of the cell holder of the spectrometer multiplied by the thickness of the cell. The number of molecules (M_2) on the SAMs can also be calculated for the same area (the area of the window of the cell holder) by using the theoretical molecular area per molecule. Assuming the absorption of the SAM is the same as that in the solution, the absorbance (A_2) of the SAM can be obtained as $A_1 \times M_2/M_1$. The absorbances obtained by this method are rather close to those of monolayer films on quartz substrates of similar fullerene derivatives prepared by the LB technique.^{13,14} The absorbances of a monolayer on quartz can be measured directly on the UV-Vis spectrometer. This indicates the reliability of the estimation method.

Results and discussion

Synthesis of the compound

The synthetic route to compounds **1–3** is shown in Scheme 1. The pyrrolidinofullerene **4** can be acylated with sebacoyl chlorides. The reaction readily stops at the monoacylated stage. The symmetrical bisfullerene derivative cannot be obtained simply by varying the ratio of **4** and sebacoyl chloride. Even when a large excess of **4** is used, the major product is still the monoacylated derivative. The preference of the dichloro-carbonyls for monoacylation of **4** provides a handy method

for attaching other substituents onto the molecule, yielding products such as **1**, **2** and **3**.

Characterization of SAMs

STM has been used to characterize fullerene thin films on a wide variety of substrates formed by evaporation of C_{60} under ultrahigh vacuum conditions.^{18,19} STM studies of fullerene-terminated SAMs on Au(111) surfaces have been reported before.^{20,21} Fig. 1 shows that very well-ordered monolayers of compounds **1**, **2** and **3** can be formed on the Au(111) surface. There is no discernible overlayer structure. These images demonstrate that the SAM of **1** has a higher coverage than SAMs of **2** and **3**. In the most densely-packed regions of these images, the fullerene-derivative moieties can be readily distinguished from each other; these results are comparable with those reported before.^{20–22}

Photoelectrochemistry

Photoelectrochemical measurements were carried out for SAMs of **1**, **2** and **3** in a 0.1 M KCl solution containing 36 mM H_2Q . Wavelengths above 400 nm were used for excitation, as the background photocurrent of bare Au slides is negligible in this region. A stable anodic photocurrent was observed. The photocurrent is stable in the presence of H_2Q and on/off switching of the light can be repeated tens of times with little attenuation (Fig. 2). Under illumination by 404 nm light (2.10 mW cm^{-2}) and in the presence of 36 mM H_2Q , anodic photocurrents of 1368, 716 and 255 nA cm^{-2} were observed for **1**, **2** and **3**, respectively.

Fig. 3 shows a typical photocurrent response as a function of excitation wavelength for the SAM of **1**. The absorption spectrum of **1** in chloroform is also shown. The two spectra are similar, indicating that the fullerene derivative **1** in the SAM is responsible for the photocurrent generation. Similar

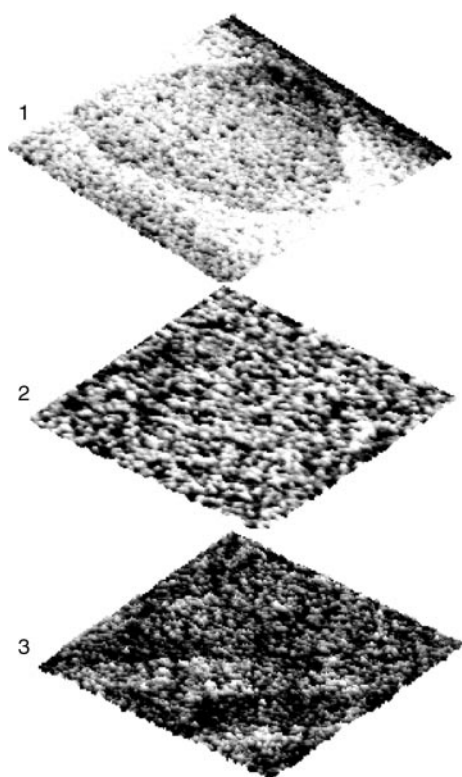


Fig. 1 STM images for SAMs of **1** ($100 \text{ nm} \times 100 \text{ nm}$), **2** ($110 \text{ nm} \times 110 \text{ nm}$) and **3** ($110 \text{ nm} \times 110 \text{ nm}$) on Au(111). The image was acquired at +1.0 V sample bias and 100 pA tunneling current. Numbers to the left of the graphs represent compounds **1**, **2** and **3**.

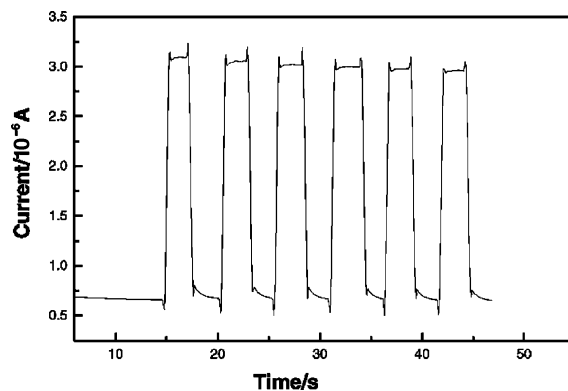


Fig. 2 Representative photocurrent obtained from SAM of **1** (0.2 V bias voltage, 36 mM H_2Q , 0.1 M KCl electrolyte solution, $\lambda = 404 \text{ nm}$, 2.1 mW cm^{-2}).

spectra were obtained for compounds **2** and **3** on the modified gold electrodes.

The relationship between the photocurrent generation of SAMs of **1**, **2** and **3** and light intensity is shown in Fig. 4. According to Donovan's theory,²³ the photocurrent depends on the irradiation light intensity through $i = KI^m$, where i is the photocurrent generated and I is the intensity of the light. $m = 1$ is characteristic of unimolecular recombination and $m = 0.5$ is characteristic of bimolecular recombination. A linear relationship between the measured photocurrent (i) and the light intensity (I) for compounds **1**, **2** and **3** was observed, indicating a unimolecular recombination mechanism for all three compounds.

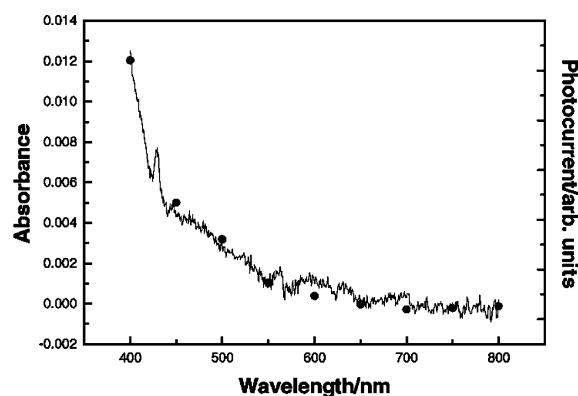


Fig. 3 Action spectrum of SAM of **1** (●) and absorption spectrum of **1** ($12.1 \mu\text{M}$) in CHCl_3 (full line).

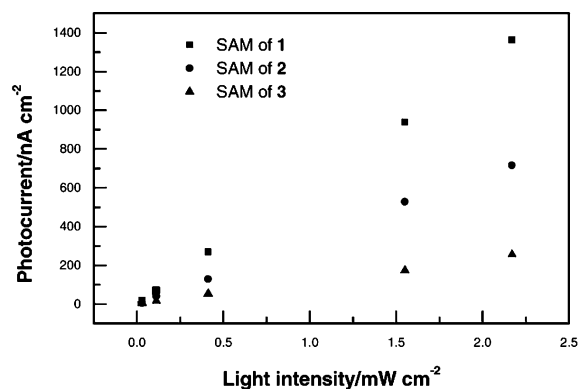


Fig. 4 The relationships between the photocurrent generation of SAMs of **1** (■), **2** (●) and **3** (▲) and light intensity ($\lambda = 404 \text{ nm}$, 0.1 M KCl, 36 mM H_2Q).

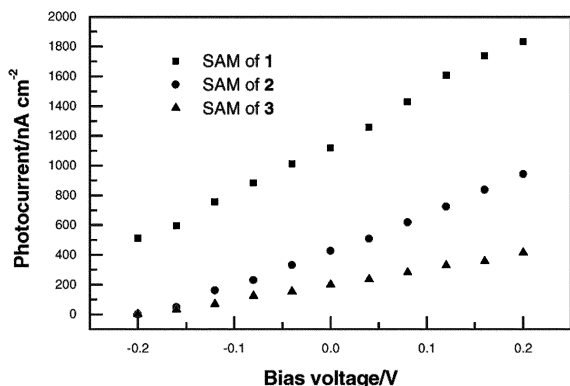
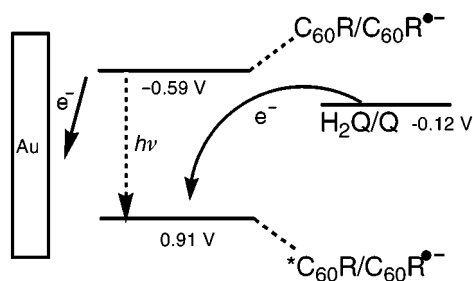


Fig. 5 The effect of bias voltage on the photocurrent generation of SAMs of **1** (■), **2** (●) and **3** (▲) (0.1 M KCl, $\lambda = 404$ nm, 2.1 mW cm^{-2} , $36 \text{ mM H}_2\text{Q}$).

The effect of bias voltage was also investigated. A linear relationship between the observed photocurrent and the bias voltage in the range -0.2 to 0.2 V vs. SCE was observed, with slopes of 3.04 , 2.13 and 0.98 nA mV^{-1} for **1**, **2** and **3**, respectively (Fig. 5). The photocurrent increases as the positive bias voltage of the electrode increases. This indicates that the applied positive voltage has the same polarity as the photocurrent, and the electrons flow from the electrolyte through the SAMs to the electrode.

Absorption spectra for SAMs of **1**, **2** and **3** could not be obtained because of the low absorption. Assuming that the absorptions of **1**, **2** and **3** on the gold surface are the same as those in chloroform²⁴ and also assuming perfect coverage of the SAMs, absorbances of SAMs of **1**, **2** and **3** are calculated to be 7.9×10^{-3} , 9.5×10^{-3} and 9.3×10^{-3} . Under excitation with $\lambda = 404 \text{ nm}$ light of 2.10 mW cm^{-2} and 0.2 V bias voltage, the optimal photocurrent density is 1820 nA cm^{-2} for **1**, 942 nA cm^{-2} for **2** and 415 nA cm^{-2} for **3**. Based on these data, we can estimate that the quantum yields of **1**, **2** and **3** are 14.9 , 6.5 and 2.9% , respectively. These values are probably slightly lower than the actual quantum yields because of the above assumption of perfect surface coverage. Compared with the quantum yields (from 3.0 to 4.8%) of C_{60} LB films,^{13,14,25} the yield of **1** is much larger. Yields of 7.5 and 0.1% have been reported for similar photoelectrochemical cells of other fullerene derivative²⁴ and porphyrin²⁶ SAMs, respectively. A ferrocene-porphyrin-fullerene SAM on Au was reported recently to exhibit a 25% yield.¹⁵

Compared with SAMs of **2** and **3**, the SAM of **1** gives higher photocurrents. This may be due to the different terminal groups of the compounds, which are the ones interacting with the Au surface. For compound **1**, its SAM on Au has Au–N bonds, whereas **2** and **3** have Au–S bonds. Compared to the sulfur-containing terminal groups of **2** and **3**, the amino pyridine terminal group of **1** is strongly electron donating. The higher coverage of the SAM of **1** may also improve the quantum yield.



Scheme 2 Schematic diagram showing the photocurrent generation mechanism in SAM of **1**.

Mechanism of photoinduced electron transfer

In order to examine the electron transfer process for the photocurrent generation, the electrochemical properties of **1–3** have been investigated. The first reduction potentials of **1–3** are at -1.05 (-0.59), -1.07 (-0.61) and $-1.04 \text{ V vs. Fc/Fc}^+$ (-0.58 V vs. SCE), respectively. It is known that the attachment of different groups onto C_{60} leads to only minor changes for the excited state energy. The reduction potentials of excited triplet states for compounds **1**, **2** and **3** can thus be calculated as 0.91 , 0.89 and 0.92 V vs. SCE , respectively.²⁴ The oxidation potential of H_2Q in 0.1 M KCl solution is at -0.12 V vs. SCE . With these data the energy level diagram in Scheme 2 can be constructed. The anodic photocurrent may arise from the following process: upon irradiation the fullerene derivatives are excited from the ground state to the triplet state, which is reduced to the anion by the electron donor H_2Q ; the resulting C_{60} anion would give an electron to the gold electrode to give back the ground state and complete the circuit for the observed anodic photocurrent.

In summary, three new fullerene derivatives were synthesized. They can form stable SAMs on Au surfaces, which can generate stable and large anodic photocurrents. The high quantum yield implies that a combination of C_{60} and SAMs is effective for initiating electron transfer.

Acknowledgement

The authors thank the Natural Science Foundation of China for financial support (Grant 29825102).

References

- H. W. Kroto, J. R. Heath, S. C. O'Brien, R. F. Curl and R. E. Smalley, *Nature (London)*, 1985, **318**, 162.
- J. W. Arbogast, C. S. Foote and M. Kao, *J. Am. Chem. Soc.*, 1992, **114**, 2277.
- D. Guldi, R. E. Huie, P. Neta, H. Hungerbuhler and K. D. Asmus, *Chem. Phys. Lett.*, 1994, **223**, 511.
- (a) D. Kuciauskas, S. Lin, G. R. Seely, A. L. Moore and D. Gust, *J. Phys. Chem.*, 1996, **100**, 15926; (b) D. I. Schuster, P. Cheng, S. R. Wilson, V. Prokhorenko, M. Katterle, A. R. Holzwarth, S. E. Braslavsky, G. Klihm, R. M. Williams and C. P. Luo, *J. Am. Chem. Soc.*, 1999, **121**, 11599; (c) H. Imahori, H. Yamada, Y. Nishimura, I. Yamazaki and Y. Sakata, *J. Phys. Chem.*, 2000, **104**, 2099.
- M. Maggini, A. Dono, G. Scorrano and M. Prato, *J. Chem. Soc., Chem. Commun.*, 1995, 843.
- D. M. Guldi, M. Maggini, G. Scorrano and M. Prato, *J. Am. Chem. Soc.*, 1997, **119**, 974.
- Y. Yoshida, N. Tanigaki and K. Yase, *Thin Solid Films*, 1996, **281–282**, 80.
- S. Wang, R. M. Leblanc, F. Arias and L. Echegoyen, *Langmuir*, 1997, **13**, 3, 1672.
- C. A. Mirkin and W. B. Caldwell, *Tetrahedron*, 1996, **52**, 5113.
- A. Ulman, *Introduction to Ultrathin Organic Films*, Academic Press, San Diego, 1991.
- O. Dominguez and L. Echegoyen, *Langmuir*, 1998, **14**, 8217.
- Y. Zhao, L. B. Gan, D. Zhou, C.-H. Huang, J. Jiang and W. Liu, *Solid State Commun.*, 1998, **106**, 43.
- W. Zhang, L. B. Gan and C.-H. Huang, *Synth. Met.*, 1998, **96**, 223.
- W. Zhang, L. B. Gan and C.-H. Huang, *J. Mater. Chem.*, 1998, **8**, 1731.
- (a) H. Imahori, H. Yamada, S. Ozawa, K. Ushida and Y. Sakata, *Chem. Commun.*, 1999, 1165; (b) H. Imahori, T. Azuma, A. Ajavakom, H. Norieda, H. Yamada and Y. Sakata, *J. Phys. Chem. B*, 1999, **103**, 7233.
- H. X. Luo, W. Zhang, L. B. Gan, C. H. Huang and N. Q. Li, *Electroanalysis*, 1999, **11**, 238.
- L. B. Gan, D. J. Zhou, C. P. Luo, H. S. Tan, C. H. Huang, M. J. Lu, J. Q. Pan and Y. Wu, *J. Org. Chem.*, 1996, **61**, 1954.
- R. J. Wragg, H. W. Chamberlain, H. W. White, W. Krättschmer and R. D. Huffman, *Nature (London)*, 1990, **348**, 623.
- J. K. Gimzewski, S. Modesti, T. David and R. R. Schlittler, *J. Vac. Sci. Technol. B*, 1994, **12**, 1942.

- 20 Y. S. Shon, K. F. Kelly, N. J. Halas and T. R. Lee, *Langmuir*, 1999, **15**, 5329.
- 21 X. Shi, W. B. Caldwell, K. Chen and C. A. Mirkin, *J. Am. Chem. Soc.*, 1994, **116**, 11598.
- 22 E. I. Altman and R. J. Colton, *Surf. Sci.*, 1993, **295**, 13.
- 23 K. J. Donovan, R. V. Sudiwala and E. G. Wilson, *Mol. Cryst. Liq. Cryst*, 1991, **194**, 337.
- 24 H. Imahori, T. Azuma, S. Ozawa, H. Yamada, K. Ushida, A. Ajavakom, H. Norieda and Y. Sakata, *Chem. Commun.*, 1999, 557.
- 25 W. Zhang, Y. R. Shi, L. B. Gan, C.-H. Huang, H. X. Luo, D. G. Wu and N. Q. Li, *J. Phys. Chem. B*, 1999, **103**, 675.
- 26 H. Imahori, H. Norieda, S. Ozawa, K. Ushida, H. Yamada, T. Azuma, K. Tamaki and Y. Sakata, *Langmuir*, 1998, **14**, 5335.